A Dual-Band Coupled-Line Balun Filter

Lap Kun Yeung, *Member, IEEE*, and Ke-Li Wu, *Senior Member, IEEE*

***Abstract*—In this paper, a new type of device called dual-band coupled-line bandpass balun filter is presented. Based on the traditional coupled-line filter theory and Marchand balun configuration, a new device with both filter-type, as well as balun-type characteristics is proposed. The new device utilizes $\lambda/4$-type transmission-line stepped-impedance resonators to achieve a dual-band operation. Besides providing a simple design procedure for the device, its working mechanism is also revealed mathematically. A prototype balun filter operating at 2.4 and 5.8 GHz has been realized using traditional printed circuit board technology to validate the proposed concept and theory, showing promising application potentials for future multiband RF wireless transceiver modules. Experimental measurements show good agreement with analytical and computer simulations.**

***Index Terms*—Balun, coupled line, dual-band filter, low-temperature co-fired ceramic (LTCC), stepped-impedance resonator (SIR).**

I. Introduction

The ever-increasing demand for advanced wireless communication applications necessitates RF transceivers operating at multiple separated frequency bands. For example, high-speed wireless local area networks (WLANs), offering up to 54-Mbit/s wireless access service, operate at both 2.4- and 5-GHz bands. To accommodate such dual-band RF signal reception and transmission, devices such as dual-band antennas, dual-band baluns, and dual-band filters are currently gaining wide attention. Among various functional passives, the filter is considered as one of the most important components and, therefore, a great deal of effort has been focused on this particular area [1]–[6], especially on the filter configuration that utilize stepped-impedance resonators (SIRs) to achieve the dual-band feature. For example, two recent publications [7], [8] have demonstrated the use of parallel-coupled microstrip lines to construct dual-band bandpass filters with fully controllable bandwidths and return losses for both operating frequency bands.

While much attention has been paid to filters, not much research has been done on the balun even though it is also a key RF front-end functional passive. A balun is a device for converting a balanced signal to an unbalanced one, or vice versa.

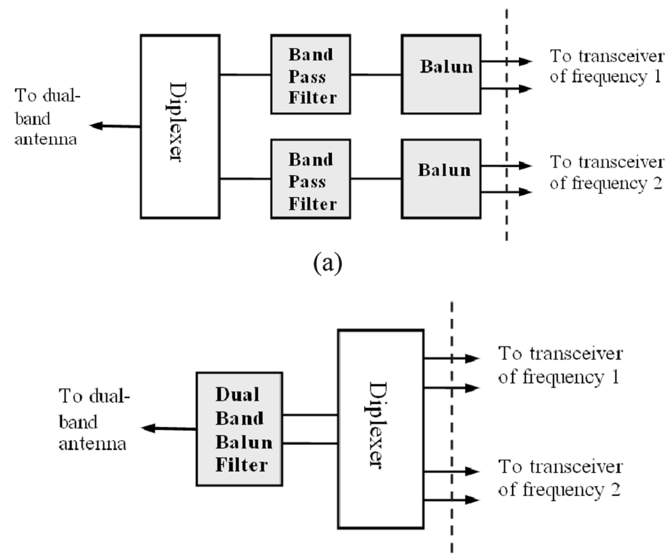

Fig. 1. (a) Architecture of a traditional dual-band RF front-end. (b) New architecture of a dual-band RF front-end using the proposed balun filter.

A balanced signal consists of two signal components with the same magnitude, but 180° out-of-phase. Many analog circuits, such as mixers, amplifiers, and multipliers, require a balanced input or output to achieve noise or high-order harmonics reduction. A dual-band balun [9] using a tapered-line structure has been recently proposed. It is essentially a conventional Marchand balun with its uniform coupled-line sections replaced by tapered counterparts.

For single-band applications, passive devices that combine both filter- and balun-type functionalities have been proposed [10]–[12] in order to miniaturize RF front-end system modules such as those for Bluetooth applications [13]. However, no such device exists for dual-band applications. In this paper, a novel dual-band balun filter is presented. It exploits three types of traditional RF components, i.e., the coupled-line filter, the Marchand balun, and the SIR, to accomplish the required functionalities.

Having had the proposed dual-band balun filter, the architecture of a traditional dual-band RF front-end, as shown in Fig. 1(a), in which one set of balun and bandpass filter is required for each frequency channel, can be greatly simplified to a new system architecture, as shown in Fig. 1(b). Such simplification will help to reduce the size and cost of a dual-band wireless system.

To provide a practical design guideline for the proposed new device, detailed design formulas based on the coupled transmission line theory are given in this paper. An experimental verification is also presented to validate the proposed concept.

Manuscript received April 20, 2007; revised August 16, 2007. This work was supported by the Research Grants Council of the Hong Kong Special Administrative Region under Grant 2150499.

L. K. Yeung is with the Department of Electrical Engineering, University of California at Los Angeles, Los Angeles, CA 90032 USA (e-mail: lkyeung@msn.com).

K.-L. Wu is with the Department of Electronic Engineering, The Chinese University of Hong Kong, Shatin, Hong Kong (e-mail: klwu@ee.cuhk.edu.hk).

Color versions of one or more of the figures in this paper are available online at http://ieeexplore.ieee.org.

Digital Object Identifier 10.1109/TMTT.2007.907402

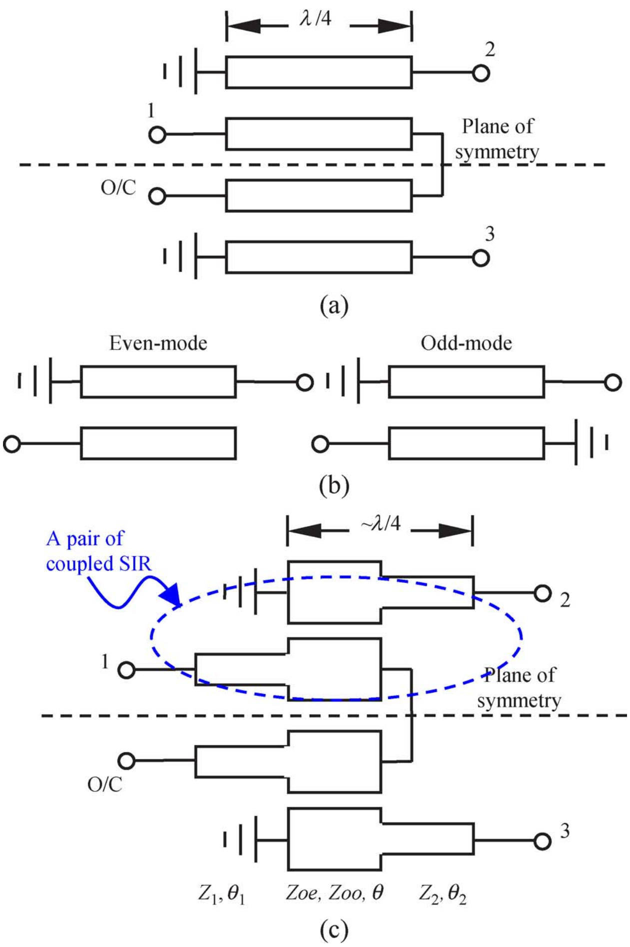

Fig. 2. (a) Conventional Marchand balun. (b) Its even- and odd-mode circuits. (c) Dual-band balun configuration.

II. Theory

A. Basic Dual-Band Configuration

A conventional Marchand balun, shown in Fig. 2(a), comprises two pairs of $\lambda/4$-long coupled-line section. It has a fairly large bandwidth and good amplitude balance, as well as 180° phase difference. According to the analysis given in [15], to satisfy the ideal balun-type characteristics of $S_{21} = -S_{31}$, the following condition is required:

$$\frac{T_{\text{even}}(1-\Gamma_{\text{odd}})}{2-(\Gamma_{\text{even}}+\Gamma_{\text{odd}})} = 0 \tag{1}$$

where Γ_{even} and Γ_{odd} are the input reflection coefficients of the even- and odd-mode circuits, respectively, and T_{even} is the transmission coefficient of the even-mode circuit. Now, looking at Fig. 2(b), the even-mode circuit of a Marchand balun presents a perfect transmission stop ($T_{\text{even}} = 0$) for all frequencies [16] and, thus, has the ideal balun-type characteristics ($S_{21} = -S_{31}$). On the other hand, when considering the return loss (S_{11}), it is sufficient to model just the odd-mode circuit, shown in Fig. 2(b). This odd-mode circuit, or the overall balun, can be made to operate at two selectable frequency bands by replacing the coupled resonator pair with a pair of coupled $\lambda/4$-type SIRs.

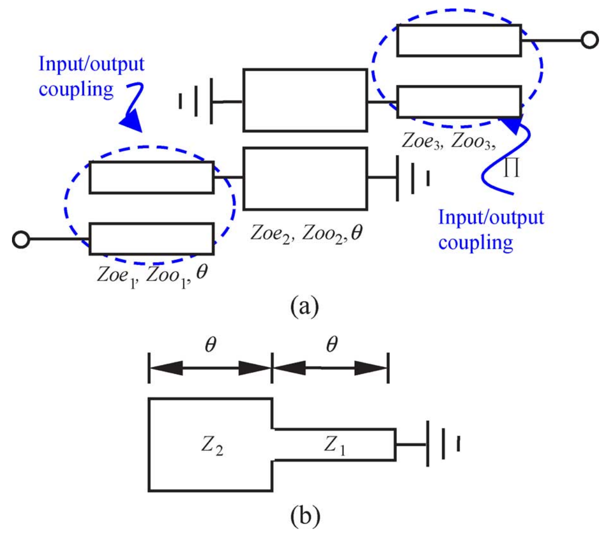

Fig. 3. (a) Modified odd-mode circuit with second-order bandpass filtering characteristics. (b) $\lambda/4$-type SIR.

With this modification, a new dual-band balun configuration is constructed, and its schematic is shown in Fig. 2(c). Only the low-impedance portion of each SIR is coupled in this example.

B. Dual-Band Balun Filter

Since the odd-mode circuit of this proposed dual-band balun resembles a pair of coupled SIRs, nth-order bandpass filtering characteristics can be introduced by simply adding extra $n-2$ resonators together with suitable input and output couplings. Without loss of generality, a second-order filtering is considered in this study [see Fig. 3(a)]. Moreover, for simplicity, the three coupling sections are assumed to have the same electrical length θ. The method for designing this filter is similar to the one described in [14], except that $\lambda/4$-type SIRs are used here.

The first step is to design a $\lambda/4$-type SIR, which resonates at desired frequencies. It can be seen from Fig. 3(b) that there are three adjustable parameters for a SIR, i.e., θ, Z_1, and Z_2. Relationships between them and the first two resonant frequencies are given by [17]

$$\frac{f_s}{f_0} = \frac{\pi}{\theta} - 1 \tag{2}$$

$$\theta = \tan^{-1}\sqrt{R_z} \tag{3}$$

where $R_z = Z_2/Z_1$ is the impedance ratio. Therefore, given two desired operating frequencies, i.e., f_0 and f_s, the impedance ratio and the electrical length of a SIR can be obtained. Additionally, its susceptance slope parameter can be calculated by

$$b = \frac{\theta}{Z_2}. \tag{4}$$

This parameter is required when designing filters using traditional filter design theory.

After obtaining a desired SIR, the odd-mode filter can be designed in a way similar to that for conventional coupled-resonator filters with some modifications. As seen in Fig. 3(a), there are two different types of coupled-line sections: the section with two open-circuit ports and the section with two short-circuit ports. The $ABCD$ matrix of the former is available and is given as [14]

$$[ABCD]_{\rm coup}^{\rm open} = \begin{pmatrix} \dfrac{Z_{oe}+Z_{oo}}{Z_{oe}-Z_{oo}}\cos\theta & \dfrac{(Z_{oe}-Z_{oo})^2+(Z_{oe}+Z_{oo})^2\cos^2\theta}{-j2(Z_{oe}-Z_{oo})\sin\theta} \\ \dfrac{j2\sin\theta}{Z_{oe}-Z_{oo}} & \dfrac{Z_{oe}+Z_{oo}}{Z_{oe}-Z_{oo}}\cos\theta \end{pmatrix} \tag{5a}$$

where Z_{oe} and Z_{oo} are the even- and odd-mode impedances of a coupled line, respectively. For the latter, its $ABCD$ matrix can be calculated as

$$[ABCD]_{\rm coup}^{\rm short} = \begin{pmatrix} \dfrac{Y_{oe}+Y_{oo}}{Y_{oe}-Y_{oo}}\cos\theta & \dfrac{-j2\sin\theta}{Y_{oe}-Y_{oo}} \\ \dfrac{(Y_{oe}+Y_{oo})^2\cos^2\theta-(Y_{oe}-Y_{oo})^2}{-j2(Y_{oe}-Y_{oo})\sin\theta} & \dfrac{Y_{oe}+Y_{oo}}{Y_{oe}-Y_{oo}}\cos\theta \end{pmatrix} \tag{5b}$$

where Y_{oe} and Y_{oo} are the even- and odd-mode admittances, respectively. To facilitate the filter design using traditional methods, each type of coupled-line section should be associated with an equivalent admittance inverter. The inverter equivalents for the section with open-circuit ports and the one with short-circuit ports are shown in Fig. 4(a) and (b), respectively. The only difference between these two equivalents is the 180° phase shift (minus sign) between their inverters. This extra minus sign is included because the odd-mode filter consists of only $\lambda/4$ SIRs, in other words, θ is equal to 45°. However, traditional admittance inverter filters require a $\lambda/2$ resonator between any pair of adjacent inverters. Therefore, an extra 90° phase shift is required on either side of the middle inverter to make the overall transmission line length between two adjacent inverters $\lambda/2$ long [see Fig. 4(c)]. The mathematical relationship between a coupled-line section and its inverter equivalent can be obtained by equating their corresponding $ABCD$ matrices. For the open-circuit case, it has been done in [14] and the results are listed as follows:

$$\frac{Z_{oe}}{Z_0} = \frac{1+(J/Y_0)\csc\theta+(J/Y_0)^2}{1-(J/Y_0)^2\cot^2\theta} \tag{6a}$$
$$\frac{Z_{oo}}{Z_0} = \frac{1-(J/Y_0)\csc\theta+(J/Y_0)^2}{1-(J/Y_0)^2\cot^2\theta} \tag{6b}$$

where Y_0 is a chosen reference characteristics admittance. For the short-circuit case, it can be obtained in the following way. Given that the $ABCD$ matrix of the inverter shown in Fig. 4(b) is

$$[ABCD]_J = -\begin{pmatrix} \left(JZ_0+\dfrac{1}{JZ_0}\right)\sin\theta\cos\theta & j\left(JZ_0^2\sin^2\theta-\dfrac{1}{J}\cos^2\theta\right) \\ j\left(\dfrac{1}{JZ_0^2}\sin^2\theta-J\cos^2\theta\right) & \left(JZ_0+\dfrac{1}{JZ_0}\right)\sin\theta\cos\theta \end{pmatrix} \tag{7}$$

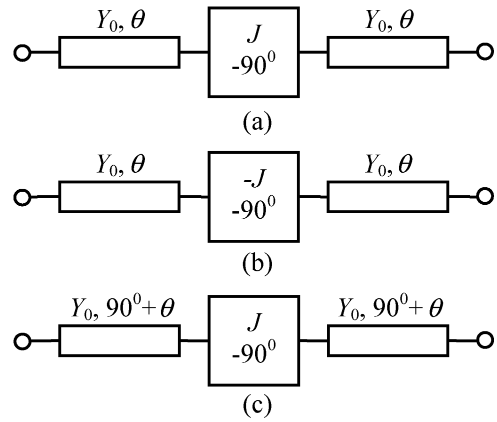

Fig. 4. Admittance inverter equivalents for: (a) coupled section with two open-circuit ports, (b) coupled section with two short-circuit ports, and (c) alternative representation for the section with two short-circuit ports.

then by equating each corresponding matrix element of (5b) and (7), we have

$$\frac{Y_{oe}+Y_{oo}}{Y_{oe}-Y_{oo}}\cos\theta = -\left(JZ_0+\frac{1}{JZ_0}\right)\sin\theta\cos\theta \tag{8a}$$
$$\frac{-2\sin\theta}{Y_{oe}-Y_{oo}} = -JZ_0^2\sin^2\theta+\frac{1}{J}\cos^2\theta \tag{8b}$$
$$\frac{(Y_{oe}+Y_{oo})^2\cos^2\theta-(Y_{oe}-Y_{oo})^2}{2(Y_{oe}-Y_{oo})\sin\theta} = \frac{-1}{JZ_0^2}\sin^2\theta+J\cos^2\theta. \tag{8c}$$

The above simultaneous equations are not independent of each other, and any two equations among these three are valid for solution. Solving the first two equations gives

$$\frac{Y_{oe}}{Y_0} = -\frac{1-(Y_0/J)\csc\theta+(Y_0/J)^2}{1-(Y_0/J)^2\cot^2\theta} \tag{9a}$$
$$\frac{Y_{oo}}{Y_0} = -\frac{1+(Y_0/J)\csc\theta+(Y_0/J)^2}{1-(Y_0/J)^2\cot^2\theta}. \tag{9b}$$

With the help of (6) and (9), the design can now proceed as usual. Herein, a set of prototype element values g_i's are chosen from standard filter design tables [18]. The admittance inverter parameters, given a relative bandwidth w, can be expressed as

$$J_{01} = \sqrt{\frac{Y_0 b_1 w}{g_0 g_1}} = Y_0\sqrt{\frac{w\theta}{g_0 g_1}}$$
$$J_{j,j+1} = w\sqrt{\frac{b_j b_{j+1}}{g_j g_{j+1}}} = Y_0\frac{w\theta}{\sqrt{g_j g_{j+1}}}, \qquad j=1,\ldots,n-1$$
$$J_{n,n+1} = \sqrt{\frac{Y_0 b_n w}{g_n g_{n+1}}} = Y_0\sqrt{\frac{w\theta}{g_n g_{n+1}}} \tag{10}$$

where $b_1, b_2, \ldots, b_n$ are the resonator susceptance slope parameters. Notice that in (10) we have assumed $Y_2 = Y_0$. Based on

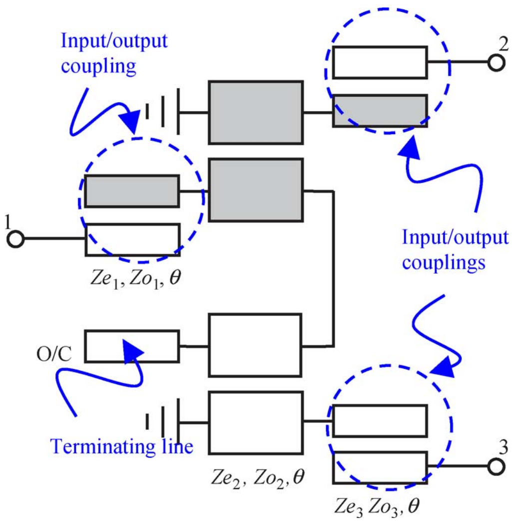

Fig. 5. Proposed dual-band coupled-line balun filter (the shaded section is a section of the partially coupled SIR coupled lines).

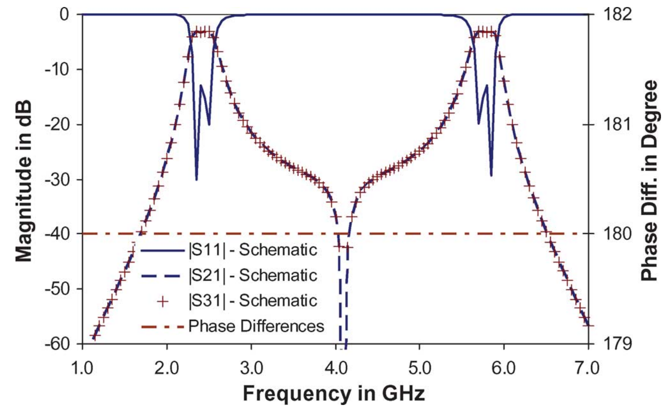

Fig. 6. Simulated responses of a dual-band balun-filter based on ideal transmission line model.

the inverter parameters, the design data for all coupled-line sections in Fig. 3(a) can be calculated and a SIR bandpass filter is thus obtained. However, for a dual-band balun-filter, extra modifications are required. Firstly, the schematic should be modified to the one shown in Fig. 5. It essentially consists of two SIR bandpass filters shown in Fig. 3(a). and each of them is a pair of coupled SIRs. Notice that the filter at the lower half has a terminating line in place of a coupled section and, therefore, this structure is not truly symmetric. However, the main body of the structure can be viewed as a dual-band balun with input and output couplings. Secondly, J_{01} should be divided by $\sqrt{2}$ because there are two filter sections in parallel. This allows the input port matches to a 100-Ω balanced load rather than a 50-Ω load, as in Fig. 3(a). Thirdly, the terminating line should be set to the chosen reference impedance Z_0 and electrical length of θ. This is because when converting the structure to an inverter equivalent, there should be no impedance discontinuity between this terminating line and the transmission line section of the inverter equivalent. Finally, it can be shown that when the frequency ratio is less than 3, the low impedance sections of the SIR resonators need to be the coupled pair.

III. Physical Implementation

The proposed balun-filter consists of five pairs of coupled-line section and a single open-circuit terminated transmission line. For those coupled-line sections, they are best realized by striplines using multilayer substrate technologies. For microstrip-type realization, however, special attention is required due to its nature of unequal even- and odd-mode phase velocities. This undesired property degrades the filter's second passband responses significantly. As an example, according to the method described above, a set of even- and odd-mode impedances has been calculated for a 300-MHz bandwidth balun filter operating at 2.4- and 5-GHz frequency bands. These impedances are $Z_{e1} = 86.74\ \Omega$, $Z_{o1} = 36.51\ \Omega$, $Z_{e2} = 31.35\ \Omega$, $Z_{o2} = 25.25\ \Omega$, $Z_{e3} = 72.61\ \Omega$, and $Z_{o3} = 38.54\ \Omega$. In addition, the characteristic impedance of the terminating line is $Z_0 = 50\ \Omega$ and all line sections have an electrical length of 52.68°. Now translating those to microstrip-type realizations on a 0.8-mm-thick FR4 printed-circuit board (PCB), the corresponding dimensions for each pair of coupled-line counted from the left end to the right end of Fig. 5 are as follows.

- *First coupled-line pair*: length = 421.48 mil, width = 29.74 mil, separation = 2.75 mil.
- *Second coupled-line pair*: length = 386.58 mil, width = 135.09 mil, separation = 20.23 mil.
- *Third coupled-line pair*: length = 413.2 mil, width = 41.67 mil, separation = 5.29 mil.
- *Terminating line*: length = 397.99 mil, width = 60.72 mil.

Fig. 6 shows the schematic-level simulations of this balun-filter using an ideal transmission line. However, the microstrip model will show a significant degradation at the 5-GHz passband due to the unequal even- and odd-mode phase velocities. Several techniques exist to overcome such problem including the use of a wiggly coupled-line section or insertion of a compensating capacitor at the middle of a coupled-line section. In our prototype, a three-conductor coupled-line section is used to alleviate this problem.

Fig. 7 shows the physical layout of our prototype filter. It is clear that there are five three-conductor coupled-line sections and an open-circuit terminated microstrip line. The tooth-like conductor printings at the center two coupled-line sections introduce extra odd-mode coupling capacitances. Moreover, for each of these sections, a conducting wire is used to connect its two outside microstrips to form a three-conductor coupled-line configuration. A photograph of the physical realization of the prototype on FR4 substrate is shown in Fig. 8.

IV. Experimental Results

The measured and full-wave simulated performances of the prototype balun-filter designed at 2.45 and 5.55 GHz are shown in Fig. 9. The wider bandwidth at the higher passband, as compared to that of the schematic circuit shown in Fig. 6, is caused by the dispersion of the coupling elements. The downward shift of the upper passband frequency of the electromagnetic (EM) simulated and measured results, as compared to the desired one in the schematic simulation, is due to the parasitic effects of the resonators. Nevertheless, this result is convincing enough

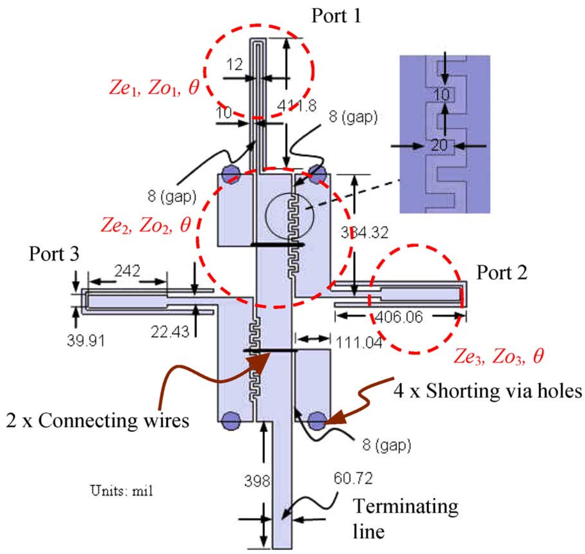

Fig. 7. Microstrip-type implementation of the proposed balun filter. (Ground is not shown. Thickness of the substrate is 31.5 mil.)

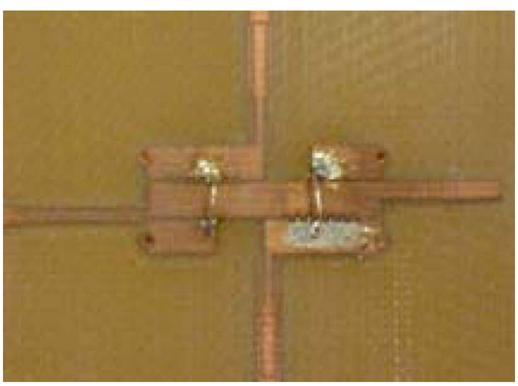

Fig. 8. Experimental prototype.

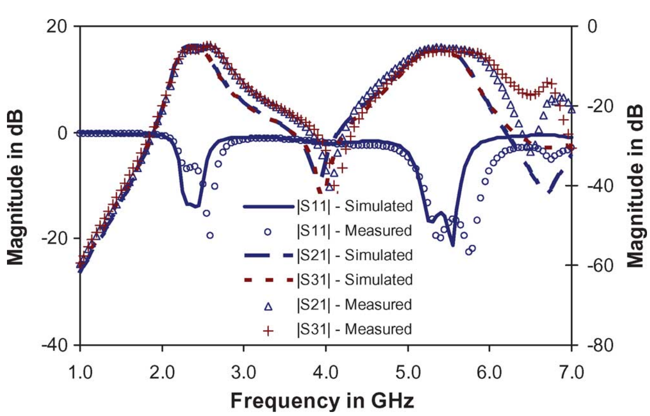

Fig. 9. Comparison between EM simulated and measured results.

to prove the concept. It is easy to adjust the higher passband to 5.8 GHz by tuning the physical layout.

Fig. 10 shows the amplitude balance and phase difference of the balun filter at each operating band. From this figure, the 2.4-GHz band has a better performance with an amplitude balance of 0.3-dB maximum and a maximum of 2° phase difference. For the 5-GHz band, the corresponding figures are 0.9 dB and 9°, respectively. Obviously, the performance at the 5-GHz band has been degraded by the previously mentioned unequal even- and odd-mode velocities of the microstrip coupled-line section. This predicament can be removed if the circuit is realized by stripline structures using such low-temperature co-fired ceramic (LTCC) multilayer technologies.

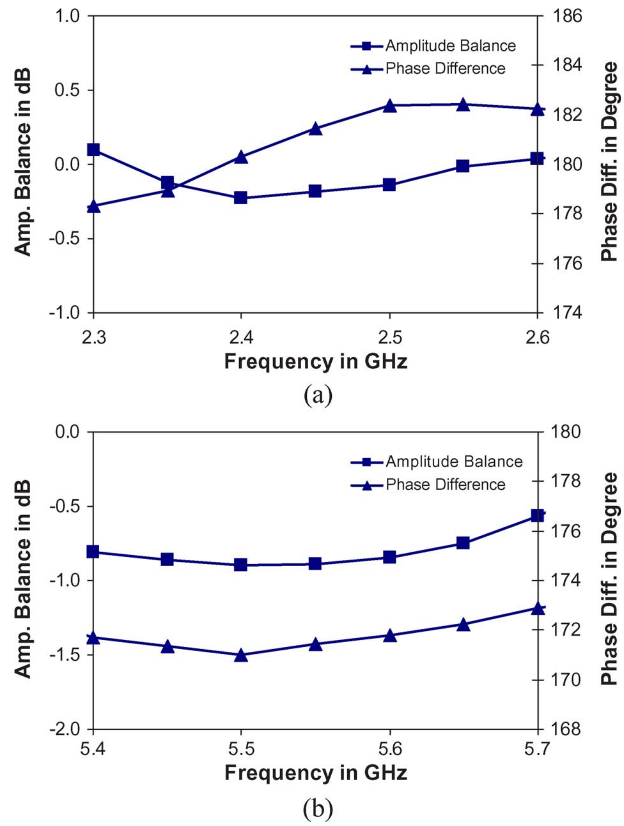

Fig. 10. Performance of the proposed balun-filter at: (a) 2.4- and (b) 5-GHz band.

V. Conclusion

The new concept of a dual-band balun filter has been presented. The concept exploits three types of traditional RF components including a coupled-line filter, Marchand balun, and SIRs to accomplish both dual-band filtering and balun-type operations. Besides presenting the fundamental theory and working mechanism, an experimental prototype has been realized to validate the proposed concept. Measured results show that the device exhibits a good amplitude balance, as well as phase difference within the two designed operating frequency bands. Whereas this balun-filter is best implemented in a stripline type format using multilayer substrate technology, it can also be implemented using traditional PCB technology in a microstrip-type format. When implemented in a PCB format, special attention should be paid to the inequality between the even- and odd-mode velocities of a microstrip coupled-line section. This inequality behavior degrades the device's performance. The method employed in this study to overcome this problem is the use of a three-conductor coupled-line section. In general, this balun filter serves as a good candidate for multiband wireless applications.

ACKNOWLEDGMENT

The authors are very grateful to Y. M. Fung, The Chinese University of Hong Kong (CUHK), Shatin, Hong Kong, for providing support in preparing the experimental prototype.

REFERENCES

[1] H. Miyake, S. Kitazawa, T. Ishizaki, T. Yamada, and Y. Nagatom, "A miniaturized monolithic dual band filter using ceramic lamination technique for dual mode portable telephones," in *IEEE MTT-S Int. Microw. Symp. Dig.*, 1997, vol. 2, pp. 789–792.

[2] C. Quendo, E. Rius, and C. Person, "An original topology of dual-band filter with transmission zeros," in *IEEE MTT-S Int. Microw. Symp. Dig.*, 2003, vol. 2, pp. 1093–1096.

[3] L. C. Tsai and C. W. Hsue, "Dual-band bandpass filters using equal-length coupled-serial-shunted lines and Z-transform technique," *IEEE Trans. Microw. Theory Tech.*, vol. 52, no. 4, pp. 1111–1117, Apr. 2004.

[4] S. F. Chang, Y. H. Jeng, and J. L. Chen, "Dual-band step-impedance bandpass filter for multimode wireless LANs," *Electron. Lett.*, vol. 40, no. 1, pp. 38–39, Jan. 2004.

[5] H. M. Lee, C. R. Chen, C. C. Tsai, and C. M. Tsai, "Dual-band coupling and feed structure for microstrip filter design," in *IEEE MTT-S Int. Microw. Symp. Dig.*, 2004, vol. 3, pp. 1971–1974.

[6] J. T. Kuo and H. S. Cheng, "Design of quasi-elliptic function filters with a dual-passband response," *IEEE Microw. Wireless Compon. Lett.*, vol. 14, no. 10, pp. 472–474, Oct. 2004.

[7] S. Sun and L. Zhu, "Coupling dispersion of parallel-coupled microstrip lines for dual-band filters with controllable fractional pass bandwidths," in *IEEE MTT-S Int. Microw. Symp. Dig.*, 2005, vol. 3, pp. 2195–2198.

[8] S. Sun and L. Zhu, "Compact dual-band microstrip bandpass filter without external feeds," *IEEE Microw. Wireless Compon. Lett.*, vol. 15, no. 10, pp. 644–646, Oct. 2005.

[9] Y. Guo, Z. Y. Zhang, L. C. Ong, and M. Y. W. Chia, "A novel LTCC miniaturized dualband balun," *IEEE Microw. Wireless Compon. Lett.*, vol. 16, no. 3, pp. 143–145, Mar. 2006.

[10] M. C. Park, B. H. Lee, and D. S. Park, "A laminated balance filter using LTCC technology," in *Proc. Asia–Pacific Microw. Conf.*, Suzhou, China, 2005, pp. 2974–2977.

[11] L. K. Yeung and K.-L. Wu, "An integrated RF balanced-filter with enhanced rejection characteristics," in *IEEE MTT-S Int. Microw. Symp. Dig.*, 2005, vol. 2, pp. 713–716.

[12] L. K. Yeung and K.-L. Wu, "An LTCC balanced-to-unbalanced extracted-pole bandpass filter with complex load," *IEEE Trans. Microw. Theory Tech.*, vol. 54, no. 4, pp. 1512–1518, Apr. 2006.

[13] L. K. Yeung, J. Wang, Y. Huang, S.-C. Lee, and K.-L. Wu, "Development of an integrated LTCC Bluetooth module," in *Proc. Asia–Pacific Microw. Conf.*, Suzhou, China, 2005, pp. 3379–3382.

[14] M. Makimoto and S. Yamashita, "Bandpass filters using parallel coupled stripline stepped impedance resonators," *IEEE Trans. Microw. Theory Tech.*, vol. MTT-28, no. 12, pp. 1413–1417, Dec. 1980.

[15] K. S. Ang, Y. C. Leong, and C. H. Lee, "Analysis and design of miniaturized lumped-distributed impedance-transforming baluns," *IEEE Trans. Microw. Theory Tech.*, vol. 51, no. 3, pp. 1009–1017, Mar. 2003.

[16] D. M. Pozar, *Microwave Engineering*. New York: Addison-Wesley, 1993.

[17] M. Sagawa, M. Makimoto, and S. Yamashita, "Geometrical structures and fundamental characteristics of microwave stepped-impedance resonators," *IEEE Trans. Microw. Theory Tech.*, vol. 45, no. 7, pp. 1078–1085, Jul. 1997.

[18] G. L. Matthaei, L. Young, and E. M. T. Jones, *Microwave Filters, Impedance-Matching Networks, and Coupling Structures*. New York: McGraw-Hill, 1964.

Lap Kun Yeung (S'00–M'02) received the B.Eng. degree in electrical and information engineering from the University of Sydney, Sydney, Australia, in 1998, the M.Eng. degree in electronic engineering from the Chinese University of Hong Kong, Shatin, Hong Kong, in 2002, and is currently working toward the Ph.D. degree at the University of California at Los Angeles (UCLA).

During 1999, he was with the Commonwealth Scientific and Industrial Research Organization (CSIRO), Sydney, Australia, where he was a research engineer involved in the numerical modeling of different antenna structures. From 2003 to 2006, he was with the Chinese University of Hong Kong, where he was involved in various LTCC multichip-module (MCM) designs and the development of numerical algorithms for analyzing multilayer embedded RF modules.

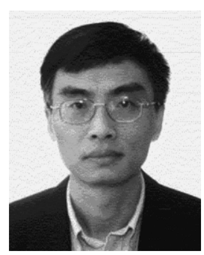

Ke-Li Wu (M'90–SM'96) received the B.S. and M.Eng. degrees from the Nanjing University of Science and Technology, Nanjing, China, in 1982 and 1985, respectively, and the Ph.D. degree from Laval University, Quebec, QC, Canada, in 1989.

From 1989 to 1993, he was with the Communications Research Laboratory, McMaster University, Hamilton, ON, Canada, as a Research Engineer and a Research Group Manager. In March 1993, he joined the Corporate Research and Development Division, ComDev International, where he was a Principal Member of Technical Staff in charge of developing advanced EM design software for passive microwave subsystems for communication satellites. Since October 1999, he has been with the Department of Electronic Engineering, The Chinese University of Hong Kong, Shatin, Hong Kong, where he is currently a Professor. He has authored or coauthored numerous publications in the areas of EM modeling and microwave and antenna engineering. His current research interests include numerical and analytical methods in electromagnetics, passive microwave circuits, filters, antennas for communication systems, LTCC-based MCMs for wireless communications, and RF identification (RFID) technologies.